*ADMET & DMPK 3(1) (2015) 51-67; doi: **10.5599/admet.3.1.169***

ADMET

**Open Access : ISSN : 1848-7718**

***http://www.pub.iapchem.org/ojs/index.php/admet/index***

*Original scientific paper*

# Adaptation of a human gut epithelial model in relation to the assessment of clinical pharmacokinetic parameters for selected tyrosine kinase inhibitors

Richard J Honeywell, Christien Fatmawati, Marita Buddha; Sarina Hitzerd, Ietje Kathman and Godefridus J. Peters*

*Dept. of Medical Oncology, VU University Medical Center, PO Box 7057, 1007 MB Amsterdam, The Netherlands*

*Corresponding author, E-mail: gj.peters@vumc.nl, tel: +3120 444 2633, fax: +3120 444 3844,*

Received: February 19, 2015; Revised: March 24, 2015; Published: March 31, 2015

***Abstract***

*The absorption, efflux and transport properties of two of the most commonly used tyrosine kinase inhibitors (TKIs), Erlotinib (E) and Gefitinib (G) were investigated using an adapted workable methodology of a 3-day Caco-2 cell monolayer transwell system, a standard model to test drug permeability and uptake of orally administered compounds. Monolayer integrity was tested using trans-epithelial electrical resistance (TEER) measurements, while drug concentrations were determined with a validated LC-MS/ MS technique. Addition of 5 % bovine serum albumin (BSA) maintained drug concentrations at ± 20 µM through the avoidance of chelate formation, (nevertheless, a reduced accumulative mass transport of the protein bound drug was observed). Investigation with Ko143 (a specific blocker of ABCG2) or $NaN_3$ (a metabolic inhibitor) indicated an interplay between active transport and to a less degree passive diffusion for gefitinib. However, for erlotinib results indicate a more dominant passive diffusion supported by one or more active transport mechanisms. The use of Ko143 suggests that ABCG2 is partially involved with accumulation of both erlotinib and gefitinib in the intestinal cell. This adapted methodology is well suited for absorption, efflux and transport studies and may be extended to investigate the dominant mechanism involved in the transport of TKIs.*

**Keywords**

Tyrosine kinase inhibitors; Caco-2, transwell; gut epithelial; gut model; drug absorption.

## Introduction

In recent years, approaches to treatment of various different oncological disorders have been directed towards the application of a series of small molecules referred to as tyrosine kinase inhibitors (TKIs). This loosely related family of molecules specifically target the tyrosine kinase domain of growth factor receptors in the cellular membrane or cytosol which play an important role in the control of cell growth and replication [1-4]. Two of the most commonly used TKIs are erlotinib (non-small cell lung cancer (NSCLC), pancreatic cancer (PC)) and gefitinib (NSCLC) [5]. Erlotinib and gefitinib both show similarity in their basic structure with a central pyrimidine core, an adenosine triphosphate (ATP)

binding side chain and a basic side chain (Figure 1). Both gefitinib and erlotinib specifically target epidermal growth factor receptor (EGFR) [6].

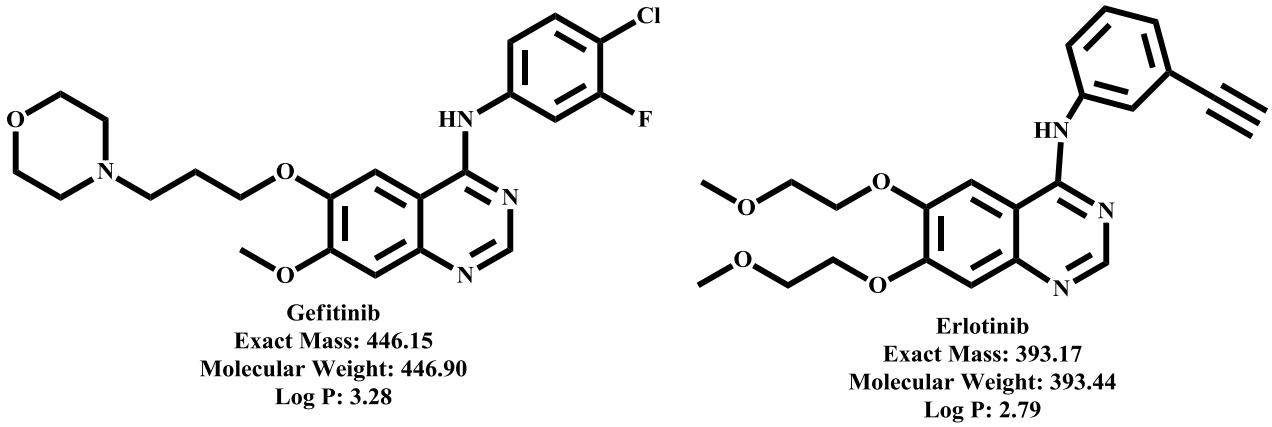


**Figure 1.** The physical and chemical properties for Gefitinib (Ge) and Erlotinib (Er). Log *P* is estimated by Viswanadhan's fragmentation [7].

TKIs represent an orally self-administered treatment that can be handled on an outpatient basis. Oral administration has a lot of beneficial aspects such as ease of use and suitability for long term treatment. However, resistance to these molecules can develop over time. This may be mediated by one of the multidrug resistance (MDR) proteins which form a group of active efflux pumps of the ATP binding-cassette (ABC) drug transporters; the pumps may catalyze the efflux of TKIs out of the enterocyte cells [8-10]. There are seven subfamilies of ABC efflux transporter (ABCA – ABCG) based on their domain structure [11]. Drug interaction with the efflux transporter as a substrate or an inhibitor depends on the concentration of drugs, for example ABCG2 may transport substrates like erlotinib and gefitinib at low concentrations (0.1 – 1 μM) [11], but shows inhibitory reaction with these drugs at higher concentrations [12-15]. The ABCG2 might transport substrates in the same way as ABCB1 that expels the drugs out of the cell or only translocate them inside of the cell [15], for which both conditions are lessening the effectiveness of treatment.

In addition to MDR, barriers to oral chemotherapy are the intestinal drug permeability uptake through epithelial cells of the inner intestinal wall, metabolism in the liver and enzymatic degradation in the intestinal tract [16]. The overall prediction of efficacy of an oral based treatment is possible by using an appropriate model system in vitro [17]. An ideal model system for intestinal absorption is based on the growth of a cellular monolayer and the careful comparison of the drug transport across this barrier. This system is referred to as a transwell system and consists of a donor, receiver and cellular compartment. Figure 2 illustrates the schematic diagram of a compartmental model and working model of a transwell system. Transport processes can occur with both a unidirectional and/or a bi-directional mechanism of either active transport by a receptor based protein system or by passive diffusion along a concentration gradient [18]. Active transport requires energy (ATP dependent) and can be against a concentration gradient, it plays a major role in the uptake of hydrophilic compounds into the cell and in the efflux of drug out of the cell. Passive diffusion from higher to lower concentration is ATP independent and occurs through lateral diffusion, transcellular or paracellular pathway [18].

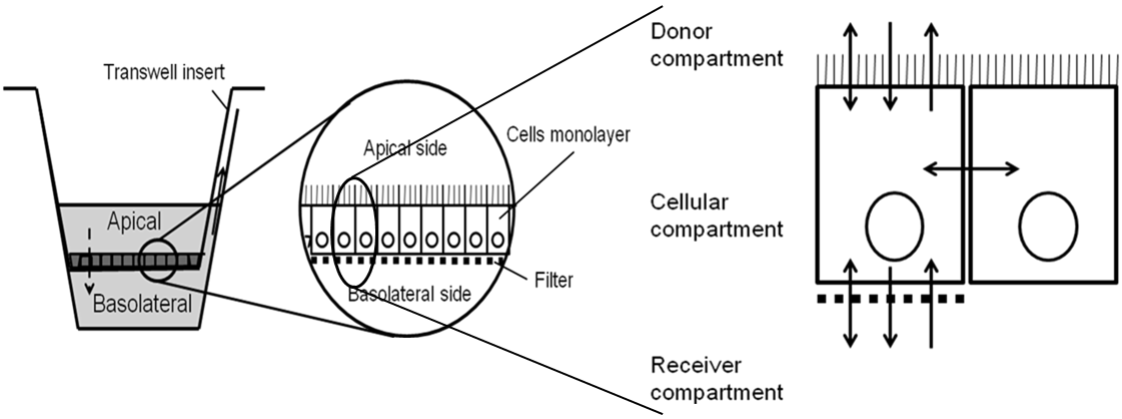


**Figure 2.** Schematic diagram of Caco-2 cell monolayer and drug transport processes in the transwell system. Apical side represents the luminal side of the enterocyte and basolateral side represents the blood circulation. The dashed arrow describes drug uptake from the apical to the basolateral side where the apical side serves as donor compartment and basolateral side serves as receiver compartment. Single headed arrows in the transport processes between compartments describe unidirectional processes while the double-headed arrows describe bidirectional processes. Drug transport between cellular compartments involves bidirectional processes.

A widely used model system consisting of a Caco-2 cell monolayer, which is a polarized cell line derived from human epithelial colorectal adenocarcinoma cells [19]. When cultured as a monolayer (in vitro), this cell line demonstrates the same phenotype, morphology and functions as enterocytes of the small intestine [20-23]. Since this cell line expresses the same enzymes and transport proteins that mediate drug uptake or efflux in the intestine, it is possible to determine significant correlation between permeability of compounds under in vivo conditions [23]. The transwell system has become the standard model to test the drug permeability and uptake of orally administered compounds [17]. Caco-2 cell monolayers enable investigation into the absorption of drugs, the passive and the active transport systems of its transport processes across a barrier directly comparable to the human system.

A disadvantage of this model system is the standard 21 day protocol for the formation of the Caco-2 monolayer [23]. An alternative 3-day culture system offers a more convenient and productive alternative that has been demonstrated to provide comparable results to the standard system [24].

We optimized this model to investigate the absorption, efflux and transport properties of two TKIs, namely erlotinib and gefitinib, utilizing LC-MSMS sensitivity to reliably measure the individual compound levels [25].

## Experimental

### *Materials*

Erlotinib and gefitinib were purchased from LC Laboratories (Woburn, MA, USA). All general reagents were purchased from Sigma (Zwijndrecht, The Netherlands). Ko143 was a kind gift of Professor GJ Koomen, University of Amsterdam, The Netherlands. Fetal bovine serum (FBS) was purchased from PAA Laboratories GmbH (Pasching, Austria) while the bovine serum albumin (BSA) fraction V was purchased from Roche Diagnostics (Mannheim, Germany). Roswell Park Memorial Institute (RPMI) 640 medium, trypsin--EDTA, penicillin, streptomycin (10000 U/ml) and 1 M Hepes Buffer (in 0.85 % NaCl) were purchased from Lonza Benelux BV (Breda, NL). Hank's balanced salt

solution (HBSS) containing $CaCl_2$ and $MgCl_2$ as the transport medium for drug transporting cross cell monolayer was purchased from Invitrogen (Breda, The Netherlands). The growth medium (Dulbecco's Modified Eagle Medium (DMEM) based), differentiation medium (a serum free medium containing butyric acid) to induce fully differentiation to enterocytes and supplemental medium to maintain the cells under serum free condition specific for Caco-2 cell monolayer were purchased from BD Biocoat™ (Breda, The Netherlands). High purity erlotinib and gefitinib was obtained from LC-Laboratories (Massachusetts, USA). Analytical grade solvents like acetonitrile, methanol and isopropanol were purchased from Biosolve BV (Valkenwaard, NL). Bio-Rad Protein Assay was purchased from Bio--Rad Laboratories GmbH (München, DE). MilliQ water was supplied via a MilliQ water purification system (Millipore, NL). All other reagents were of an analytical grade unless stated and sourced locally.

*Equipment*

The BIOCOAT® HTS Caco-2 Assay System and BD FalconTM 24-well Multiwell Plates were purchased from Becton Dickinson BV (Breda, NL). Breathe-Easier microplate sealing film was purchased from Diversified Biotech BV (Ulvenhout, NL). The microplate reader was provided by Tecan Benelux BVBA (Giessen, NL) and SPECTRA Fluor software (XFluor4 version V 4.50) was used. The Trans Epithelial Electrical Resistance (TEER) meter (Millicell® – ERS) was provided by Millipore (Amsterdam, NL). The liquid chromatography coupled to mass spectrometry (LC-MS/MS) analyses were performed using a Dionex Ultimate 3000 system coupled with an API 3000 mass spectrometer. For this system the following software was used; Analyst version 1.5.2 from Applied Biosciences, in combination with Dionex, Chromeleon LC modules version 6.8, controlled by Dionex Mass link (DMS) version 2.10 .

*Cell Culture*

The transwell system was developed using the wild type Caco-2 cell line (passage 15 – 25) after defrost. Cells were cultured routinely in DMEM containing 4.5 g/ liter glucose and L-glutamine supplemented with 10 % FBS and 20 mM of HEPES at standard conditions of 37 °C, 5 % $CO_2$ and 100 % humidity. Confluent cells were detached using trypsin EDTA and past twice weekly. Cells were seeded at a density 6.6 x $10^5$ cells/ $cm^2$ on a Biocoat 24 well transwell plate (1 µm pore size, 0.31 $cm^2$ surface area) pre-wetted with 50 µl of growth medium for 5 – 10 minutes prior to seeding. Plates were incubated for 20 – 24 hours with growth medium and then for 44 – 48 hours with differentiation medium at standard conditions. Both media were enriched with the supplemental medium (1:1000) and with 1 % Penicillin/ Streptomycin while maintaining conditions for growth and differentiation as specified by the supplier's protocol. In addition, the plate was covered with Breathe-Easier cell culture foil during incubation period to maintain identical environmental conditions for each well.

*Monolayer Integrity – Transepithelial Electrical Resistance (TEER)*

The development of a good integrity monolayer on semi-permeable filters in the transwell system is the initial crucial step prior to any drug uptake and/or transport investigation. Transepithelial electrical resistance (TEER) measures the ion permeability through the paracellular pathways and is used to determine the "intactness" of each grown monolayer. The benefit of TEER is the speed of measurements and the accuracy with which the integrity can be measured.

To this end transport medium was prepared on the day of treatment by buffering HBSS; pH 7.4 with 25 mM HEPES and 0.35 g/ litre $NaHCO_3$ [23] then adjusted to pH 7.4 with NaOH. Within the transwell plate the differentiation medium was replaced with prepared transport medium (apical - 300 µl and basolateral - 1 ml) and incubated for 15 minutes with gentle agitation (100 rpm) under

standard conditions. TEER was determined using the potential difference between two electrodes suspended across the monolayer. Measurement between each well was performed after a short washing period of the electrodes in ethanol then transport medium. The resistance measured for each monolayer before and after the experiment was adjusted by a blank resistance determined from the wells without a monolayer and multiplied by 0.31 $cm^2$ (the area of effective membrane diameter). A cut off value of 600 – 1600 Ω $cm^2$ was used for determining monolayer integrity according to specifications obtained from BD BioCoat™.

*Transport Studies*

Transport studies of 20 µM Erlotinib and Gefitinib were performed in the direction apical to basolateral (A - B) and in the direction basolateral to apical (B - A). Inhibition of cellular pump function was investigated with either 200 nM Ko143 or 1 mM $NaN_3$. Wells were pre-incubated under standard conditions for 20 minutes with 400 nM Ko143 or 1 hour with 3 mM $NaN_3$; gentle agitation (100 rpm) was applied during the incubation. All drugs were dissolved in transport medium either containing 5 % BSA or containing 5 % BSA + 1 mM $NaN_3$ and added to the donor compartment either apical (300 µl) or basolateral (1 ml). The initial concentration of the drug was verified from a 20 µl sample taken immediately from the donor compartment after drug administration (t = 0). Subsequently, samples (50 µl) were taken from each receiver compartment at the time points 15, 30, 60, 90, 120 and 180 minutes after drug administration. Following each sampling, the volume of sample taken was replaced by the same amount of pre-warmed transport medium. The plate was incubated with gentle agitation (100 rpm) at standard conditions between each time point. A final sample of 20 µl was taken from the donor compartment after 180 minutes. All samples were placed in pre-labelled tubes, stored on ice temporarily during the experiment, snap frozen in liquid nitrogen and stored at -80°C until required for analysis. After the final sample time point, cells were washed, trypsinized and harvested; the pellets were stored at -80 °C until analysis.

*Liquid Chromatography Analysis*

Extractions for chromatographic analysis of standard and samples were all performed on ice as detailed. Analysis of samples taken from the donor and receiver compartments as well as the prepared cell pellet was performed by LC-MS/ MS techniques. A simple extraction procedure of protein precipitation with acetonitrile was performed for each sample and standard preparation as reported previously [25]. LC-MS/ MS analysis was performed with a mobile phase consisting of acetonitrile, ammonium acetate (20 mM, pH 7.8) and methanol in the ratio of 66.1:24.5:8.3 % (v/v) with 1 % isopropyl alcohol added as a chromatographic modifier. Chromatographic separation was obtained with a Phenomenex prodigy ODS3 column, 3 µm particle sizes, 100 x 2.00 mm (Phenomenex, the Netherlands) at a flow rate of 0.2 ml/ minute. All mobile phases were filtered through a 0.2 µm Sartorius membrane filter and degassed for 5 minutes under vacuum with sonication.

*Calculation and Statistics*

The permeability coefficient ($P_{app}$) represents a measure for the efficiency of transport and was calculated using the total drug concentration per sample well with the following equation:

$$P_{app} = \frac{\Delta Q}{\Delta t} x \frac{V}{C_0.A}$$

where $\Delta Q/\ \Delta t$ = the rate of increase in drug concentration (accumulative mass transport) in the receiver compartment over time (µM/ second), V = volume in the receiver compartment (ml), C0 = the initial concentration of drug in the donor compartment (µM), and A = the membrane surface area ($cm^2$).

The efflux ratio was calculated according to the equation:

$$\text{Efflux ratio} = \frac{P_{app}B \rightarrow A}{P_{app}A \rightarrow B}$$

Efflux ratios > 1 indicate that drug efflux occurred during the drug transport experiment. The Papp ratios are shown as a mean value of three or more measurements ± SEM. Statistical significance was determined using a simple Student's t-test where a p value of < 0.05 was considered significant.

**Results and Discussion**

*Methodology Development*

Drug concentration

To establish a baseline for the proposed transwell transport studies a plate with no prepared monolayer was used as a control system. Either erlotinib or gefitinib was placed in the donor compartment dissolved in medium. However, control samples taken from the donor compartment medium revealed a curious decrease in concentration over time (Table 1). A drug concentration of 20 µM had been added to the donor compartment, but the actual concentration measured after the 3 hr experiment was repeatedly lower than expected, gefitinib by 1.5 fold and erlotinib by 2 to 3 fold. The observed decrease was not related to the added stock solution since analysis of this gave the correct concentration and the amount transported to the receiver compartment was negligible compared to the change observed. TKIs of this type are extremely insoluble in aqueous solutions (HBSS buffer in this instance) and are known systemically to be 90 – 100 % bound to plasma protein [6]. Therefore it was investigated whether the drug solubility was the issue behind the decreasing drug concentrations. Analysis of drug concentration in the prepared medium immediately after dilution showed concentrations in the 20-21 µM range.

**Table 1.** Apical concentrations of Erlotinib and Gefitinib (without BSA) after 0 and 3 h's in medium under standard conditions of 37 °C, 5 % $CO_2$ and 100 % humidity (n=4).

| | Donor concentration (µM) | Apical 0 hour (µM ± SEM) | Apical 3 hour (µM ± SEM) |
|---|---|---|---|
| **Erlotinib** | 20 | 10.1 ± 0.2 | 7.1 ± 0.03 |
| **Gefitinib** | 20 | 19.2 ± 0.3 | 14.8 ± 0.7 |

However, the same solution demonstrated a similar decrease in concentration after 24 hours as compared to the 3 hours post experimental sample. The lowering of the TKIs' concentration was investigated by LC-MS/ MS and complexes were observed that could be linked to the chelation of the TKIs to the metal ions in the HBSS buffer, $Mg^{2+}$ and $Ca^{2+}$ (data not shown). It was determined that

these compounds will form chelation complexes in the ratios 2:3 for gefitinib and 1:2 for erlotinib, these complexes were not broken up during sample preparation and hence the relative concentration of drug appears to decrease over time. To prevent chelation, bovine serum albumin (BSA) was added to the transport medium at a concentration of 5 % v/v, subsequently measured concentrations after 3 hours at 37 °C matched the expected concentration of 20 µM for both Erlotinib and Gefitinib (Figure 3). In addition, it was also determined that the addition of $NaN_3$ or Ko143 to the transport medium did not significantly affect the initial and post donor concentrations of either Erlotinib or Gefitinib when 5 % BSA was added.

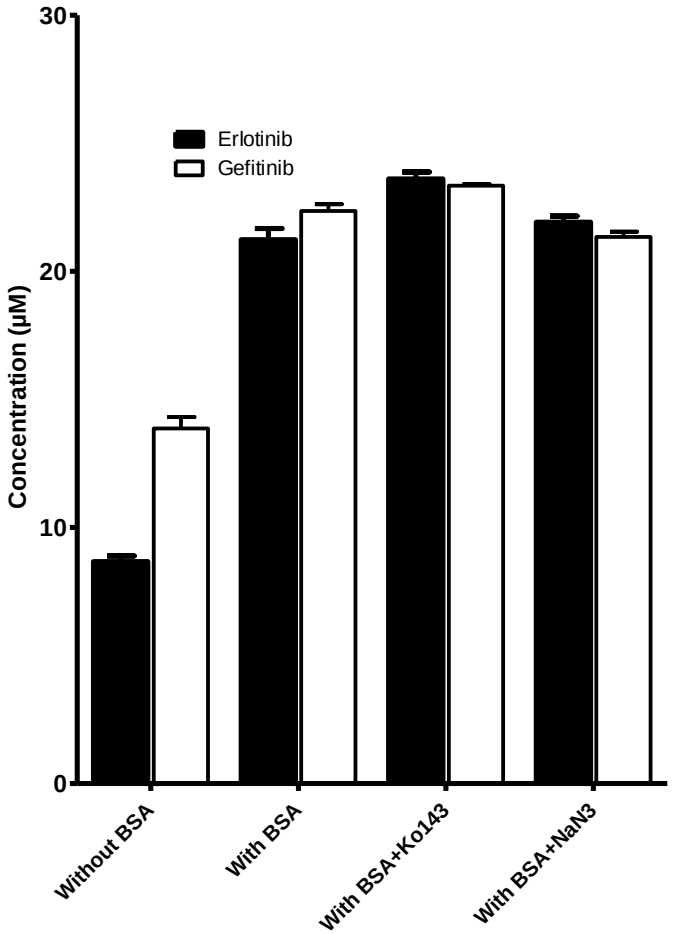


**Figure 3**. Comparison of the concentration determined for prepared 20 µM solutions of Erlotinib or Gefitinib in HBSS buffer after 3 hours at 37 °C with and without 5 % bovine serum album – (BSA). Addition of BSA prevented chelation of both Erlotinib and Gefitinib during the course of the 3 hour experimental procedure which was not affected by the addition of Ko143 or Sodium Azide. (µM ± SEM of n=16).

Using these conditions the transport over the blank transwell system (no-monolayer) was determined. Samples were taken from the receiver compartment on the same time schedule as the proposed experimental procedure. Figure 4 shows the graphical representation of the transport characteristics of gefitinib under these conditions. Linear transport characteristics are observed with both conditions. Post experiment each donor well was drained and washed three times with fresh medium. Using a 1 % DMSO solution of ethanol each used compartment was washed and the effluent collected. Analysis of the effluent revealed no evidence Gefitinib remaining on the compartment surfaces (data not shown).

Transwell monolayer reproducibility

Cells were prepared as a monolayer using a 3-day culture protocol by Yamashita et al [24] supplied as a commercial kit by Becton Dickinson BV (the Netherlands). Monolayer integrity was determined by TEER measurements prior to and after 3 hours post addition of the drugs. Values such as 260 ± 65 Ω $cm^2$ [23] and 300 – 600 Ω $cm^2$ have been quoted in literature as being a specification cut-off. [26] However, under 300 Ω $cm^2$ we observed transport characteristics that were similar to a well with no monolayer while above 1600 Ω $cm^2$ transport characteristics were highly different in regards to mass transported. Hence, the specifications for monolayer integrity was set in the range 600 – 1600 Ω $cm^2$, this was in agreement with the technical information as supplied by Becton Dickinson.

Initial TEER values revealed a problem to the formation of consistent monolayers linked to the well position within each 24 well plate. Wells closer to the sides of the plate often had TEER values indicating an incomplete monolayer, whereas more centrally placed wells were within the approved specification, indicating a complete monolayer. It was observed that Caco-2 monolayers were highly sensitive to minor fluctuations in temperature, humidity and $CO_2$ content; these fluctuations affected individual wells depending on the plate orientation and position within the incubator. To regulate the environment within each well a breathable membrane seal was applied, this was sufficient for reproducible monolayers across the entire plate to be formed within the 3-day growth period.

An additional problem was observed with the TEER measurements post experiment, here TEER values of 300 Ω $cm^2$ or lower were observed indicating loss of monolayer integrity at an unknown stage during the experimental procedure. Post experiment each well was carefully washed free of drug containing medium with the intention of recovering as many cells as possible for accumulation analysis. Additionally this washing step was included since it was unknown whether the added drugs to the medium would affect the TEER measurements. However, this washing step disrupted the monolayer significantly giving the “out of specification” TEER values. Avoiding the final washing stage TEER values demonstrated good integrity over the course of the 3 hour experiment for all the wells tested both with and without the addition of the drugs under investigation (table 2) Recovered cells were subsequently washed during the recovery process.

**Table 2.** *Good monolayer integrity was indicated by TEER value in the range of 600 – 1600 Ω $cm^2$. Each box represents one well in the transwell plate. The grey boxes indicate the wells without monolayer (blank). The TEER measurements were performed before and after the experiment of transport studies.*

| | 1 | 2 | 3 | 4 | 5 | 6 |
|---|---|---|---|---|---|---|
| A | 1016.8 | 1674.0 | 1246.2 | 737.8 | 62.0 | 62.0 |
| B | 1109.8 | 905.2 | 1271.0 | 713.0 | 651.0 | 688.2 |
| C | 883.5 | 1153.2 | 1023.0 | 1147.0 | 744.0 | 775.0 |
| D | 1240.0 | 1550.0 | 1209.0 | 1581.0 | 1612.0 | 781.2 |

Referenced literature recommended 500 µl as the sampling volume from the receiver compartment, replacing volume taken at each time point with fresh drug free medium at the correct temperature [23]. In initial plates post experiment TEER values revealed that in many cases monolayer integrity was compromised with values both lower and higher than specification. Subsequent analysis of the receiver compartment samples showed abrupt changes in mass transport, increasing for TEER values under specification but decreasing for TEER values above specification. These abrupt changes were not observed in wells with consistent TEER values prior to and post drug addition. The problem was associated with the mixing of the media in the receiver compartment after sampling. It was concluded that hydrostatic pressure from pipette aspiration could either induce stress on the monolayer causing a break in integrity or introduce air bubbles from poor technique into the pores of the filter under the monolayer. This isolated the monolayer from the receiver compartment, thereby decreasing mass transport noticeably. A broken monolayer exhibited a decrease in its TEER value, but air bubbles increase the electrical resistance across the monolayer artificially elevating the subsequent TEER values. The 500 µl of sample was initially taken to provide sufficient material for extraction and analysis of each drug but caused serious problems with the monolayer. Therefore, analytical procedures were developed to reduce the amount of sample required for analysis down to 20 µl while maintaining analytical sensitivity. Hence it became possible to reduce the sample volume taken on each time point to 50 µl, this provided sufficient sample for analysis and additional volume for unforeseen analytical problems. The reduced sample volume decreased the chances that air could get under the well insert and decreased the hydrostatic pressure seen with the 50 % liquid replacement technique.

Verification of Transport with Gefitinib and Erlotinib

The transport of gefitinib across the transwell system without a monolayer established a baseline for passive diffusion across the experimental setup. The subsequent sampling procedure dictated the calculation methodology; each 15 minute sample dilutes the well concentration by a factor of 0.02. Therefore, absolute mass is determined at each time point, adjusted for sample dilution and used as the baseline value for each subsequent increase in mass to the next time point. Addition of absolute mass transport for each following time point gave the total mass transported. In this way absolute mass transported can be determined for all the time points and the $P_{app}$ calculated. Transport decreased significantly when an intact monolayer was used consistent with expectations (Figure 4). This could be explained when taking into account the chelation complex being formed in both the donor and receiver compartments, reducing the total drug being measured by the highly specific LCMSMS technique.

Comparison of the accumulated mass transport for gefitinib with and without the addition of BSA also demonstrated a clear trend (Figure 4). With the addition of BSA a decrease in the relative amounts transported across the monolayer was observed (693.8 pmol vs 473.9 pmol, t=3 hr). This could be explained by the high protein binding properties of gefitinib which would decrease the availability of the drug for transport across the membrane. All remaining experiments were performed with medium containing 5 % BSA in both the apical and basolateral compartments.

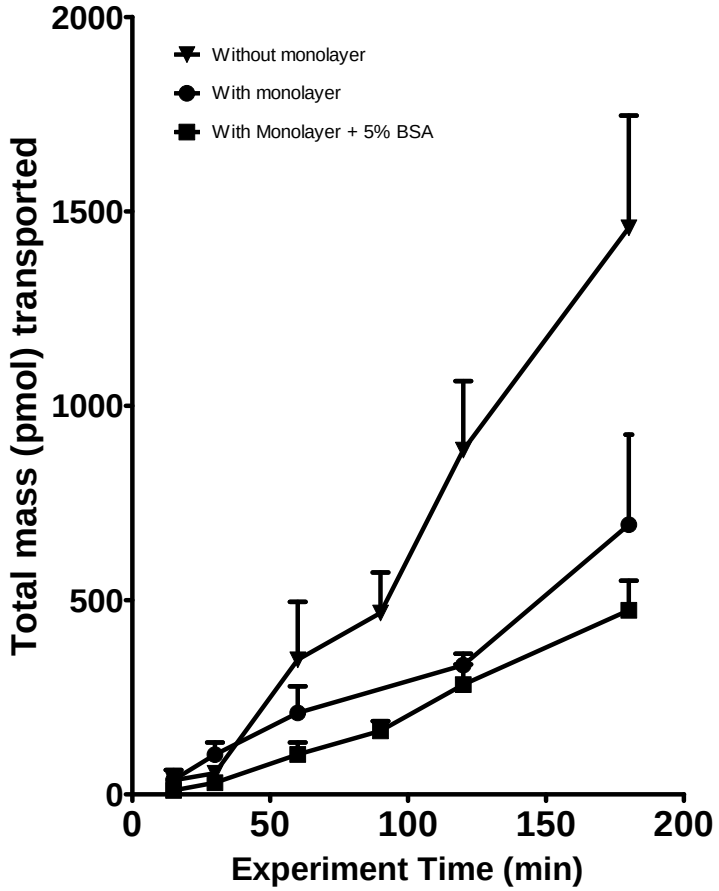


**Figure 4.** Graphical representation of transport characteristics of Gefitinib (n=4) with and without a monolayer across the Transwell setup. Where the medium (HBSS buffer) did not include BSA the total mass transported would have been affected by chelation of gefitinib with either calcium or magnesium reducing the measurable drug concentrations significantly. Addition of a monolayer to the system slows transport hence total accumulated mass while further addition of 5 % BSA also would slow transport lowering the total accumulated mass as well.

*Model Pharmacokinetic absorption*

Apical to Basolateral (A - B)

Accumulative mass transport of Gefitinib in the apical to basolateral direction (Figure 5) showed a clear linear increase over the time period measured ($P_{app}$ of 0.38 ± 0.05 µm/ s). When sodium azide ($NaN_3$) was added to the system all ATP dependent transport processes would have been blocked. In this situation gefitinib showed decrease in the observed mass transported ($P_{app}$ of 0.32 ± 0.018 µm/s) while an even greater decrease was observed when using the specific ABG2 blocker Ko143 ($P_{app}$ of 0.26 ± 0.013). Passive transport mechanisms would not be affected by $NaN_3$ but all active mechanisms would, similarly Ko143 would not inhibit passive diffusion but all mechanisms involving the ABCG2 transporter would be inhibited. Therefore it can be concluded from this evidence that gefitinib demonstrated evidence of a partial role for active transport mechanisms that occur alongside more passive mechanisms.

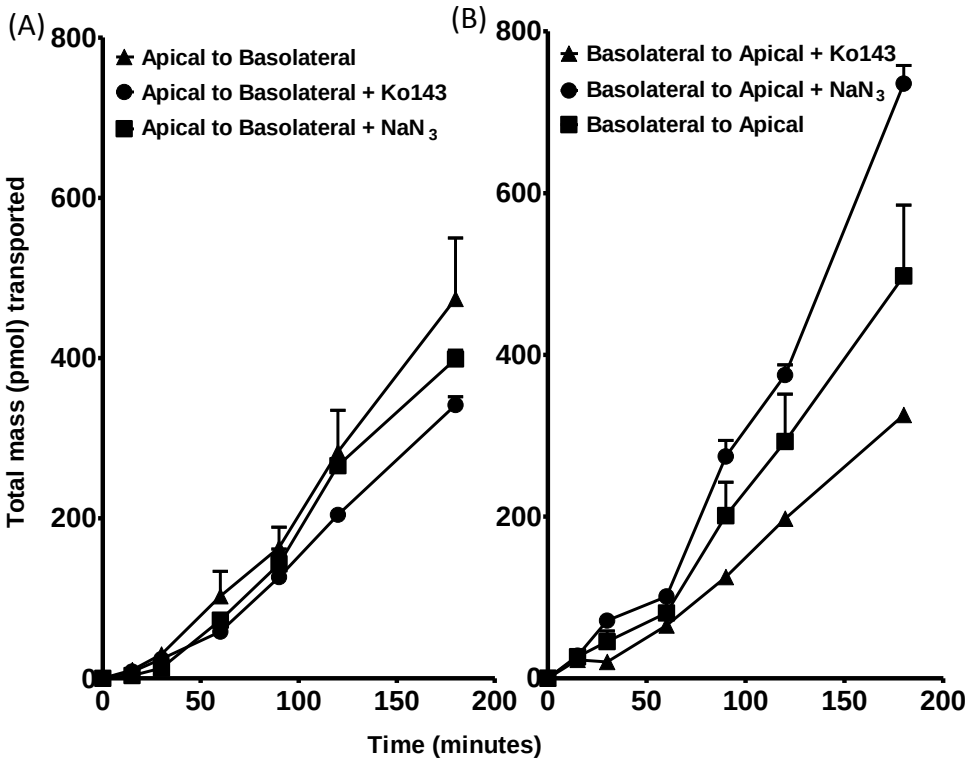


**Figure 5.** Graphical representation of accumulated drug transport in the apical to basolateral (A) and the basolateral to apical (B) directions for gefitinib using HBSS medium containing 5 % BSA. Interference in total accumulated transport is demonstrated using Ko143 (ABCG2 inhibitor) and $NaN_3$ (inhibitor of ATP processes).

Erlotinib (Figure 6) demonstrated a similar linear increase over the time period to gefitinib but at 4 - 4.5 fold higher concentrations ($P_{app}$ of 1.72 ± 0.08 µm/ s). With the addition of $NaN_3$ erlotinib had an increase in mass transported ($P_{app}$ of 2.06 ± 0.15 µm/ s), however, this was not significantly different to the transport flow without $NaN_3$. The limited effect of $NaN_3$ on the transport of Erlotinib across the membrane suggested that erlotinib transport is predominantly a passive system. However, with the addition of Ko143 a decrease in mass transported was observed that was significantly different to the control condition ($P_{app}$ of 1.23 ± 0.06, p> 0.05). This suggested that an active mechanism was involved but was an elimination mechanism on the apical membrane only.

**Table 3.** Summary of the $P_{app}$ values in both A-B and B-A directions for erlotinib and gefitinib, with and without the inclusion of the inhibitors Ko143 and $NaN_3$.Statistical comparisons were made using paired students t-test (#) comparing the $P_{app}$ A-B to the $P_{app}$ B-A. Additional comparisons were made (*) between the control and either the addition of Ko143 or $NaN_3$

| Gefitinib (n=9) | $P_{app}$ (A-B) | $P_{app}$ (B-A) | Efflux Ratio |
|---|---|---|---|
| Control | 0.38 ± 0.05 µm/s | 0.39 ± 0.038 µm/s | 1.03$^{\#}$ |
| +Ko143 | 0.26 ± 0.013 µm/s** | 0.26 ± 0.012 µm/s** | 1.00$^{\#}$ |
| +$NaN_3$ | 0.32 ± 0.018 µm/s* | 0.57 ± 0.14 µm/s** | 1.78$^{\#\#}$ |

| Erlotinib (n=12) | $P_{app}$ (A-B) | $P_{app}$ (B-A) | Efflux Ratio |
|---|---|---|---|
| Control | 1.72 ± 0.08 µm/s | 4.51 ± 0.16 µm/s | 2.62$^{\#\#\#}$ |
| +Ko143 | 1.23 ± 0.06 µm/s** | | |
| +$NaN_3$ | 2.06 ± 0.15 µm/s* | | |
| Where * or $^{\#}$ - Not significant Paired students t-test<br>** or $^{\#\#}$ - significantly different (p>0.05) paired students t-test<br>*** or $^{\#\#\#}$- Highly significantly different (p>0.01) paired students t-test | | | |

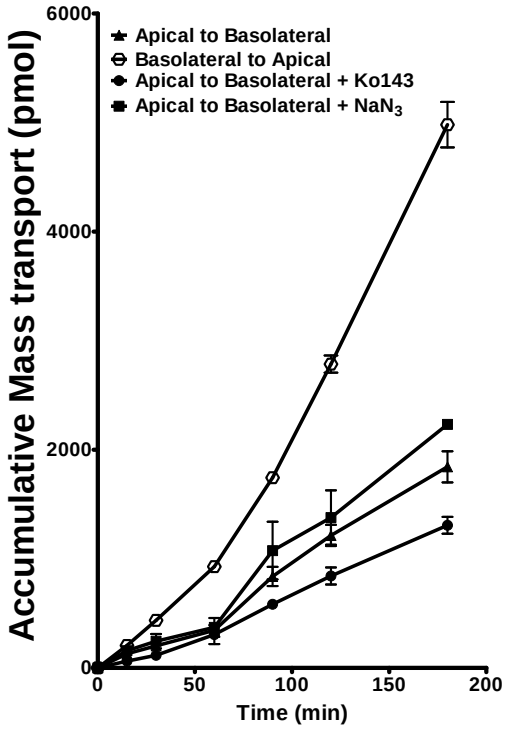


**Figure 6.** Graphical representation of accumulated drug transport in the apical to basolateral and the basolateral to apical direction for erlotinib using HBss medium containing 5 % BSA. Interference of the ATP based active transport mechanisms is demonstrated using $NaN_3$ and Ko143.

Basolateral to Apical (B - A; +5 % BSA)

To correctly interpret the pharmacokinetic properties of these drugs as determined using the model in the apical to basolateral direction, transport from the blood or cellular situation back to the epithelial side of the membrane was also investigated.

Gefitinib demonstrated very similar flow characteristics in the B - A ($P_{app}$ 0.39 ± 0.038 µm/ s) direction compared to A – B (Figure 5). However, with the addition of $NaN_3$ the flow of gefitinib increased significantly ($P_{app}$ – 0.57 ± 0.14 µm/ s, p > 0.05), whereas with the addition of Ko143 the flow decreased significantly ($P_{app}$ – 0.26 ± 0.012 µm/s, p>0.05). The net efflux ratio of gefitinib was determined to be less than 2 (1.0) which indicates a predominate flow in the basolateral to apical direction. With the introduction of $NaN_3$ the efflux ratio decreased (0.46) indicating a significant role of several active ATP transport mechanisms on both the apical and basolateral membranes in the uptake of gefitinib.

For erlotinib the B - A transport was significantly greater in comparison to A - B ($P_{app}$ – 4.51 ± 0.16 µm/ s vs $P_{app}$ – 1.72 ± 0.08 µm/ s, p > 0.009) indicating a very strong apical efflux flow as suggested by the data for the apical to basolateral flow.

Cellular accumulation of Erlotinib and Gefitinib

Analysis of cellular accumulation for each drug was performed in the cell pellet after completion of the transport studies experiment (Table 4). The accumulation of gefitinib was consistent for both A-B and B-A transport mechanisms observed during the Transwell investigation. For A-B transport gefitinib accumulation was 792.3 pmol/ mg protein which was lower than the accumulation seen for B-A transport (2059.0 pmol/ mg protein) indicating either a decreased uptake via the basolateral layer

compared to the apical or a decreased efflux via the apical layer compared to the basolateral. Addition of $NaN_3$ to the A-B donor compartment during transport slightly reduced cellular accumulation (22.9 %); while the addition of Ko143 had a more significant lowering effect (45.5 %). For B-A transport addition of $NaN_3$ led to a similar decrease in accumulation (28 %) but Ko143 had a significantly lower difference in accumulation (17.8 %). These results indicate that the measured $P_{app}$ for gefitinib transport is due to a combination of both passive and multiple active processes located on differing membranes.

**Table 4.** The cellular accumulation of gefitinib and erlotinib. Concentration of drug was determined in the recovered cells of the monolayer at the end of the transwell experiment (180 min).

| | **Gefitinib (pmol / mg protein)** | | **Erlotinib (pmol / mg protein)** | |
|---|---|---|---|---|
| | **A – B** | **B – A** | **A – B** | **B - A** |
| **Control (20 µM)** | 792.3 ± 178.8 | 2059 ± 256.5 | 741.1 ± 88.8 | 674.6 ± 71.6 |
| **20 µM + Ko143** | 431.7 ± 165.7 | 1692 ± 242.6 | 451.6 ± 81.7 | No Data |
| **20 µM + $NaN_3$** | 611.3 ± 106.2 | 1475 ± 156.9 | 835.8 ± 44.2 | |

Erlotinib demonstrated a similar accumulation in both A-B and B-A directions without addition of any inhibitors. With the addition of $NaN_3$ to the apical compartment during A-B transport an increase in cellular accumulation is seen (12.8 %), in contrast the addition of Ko143 reduced the cellular accumulation similar to that of gefitinib (39.1 %).

**Discussion**

In this paper we described the optimization and validation of a Caco-2 gut epithelial model system in order to simulate uptake characteristics of the family of compounds classified under the name of Tyrosine Kinase inhibitors. This series of small molecule inhibitors have demonstrated strong in vitro chemotherapy potential but many exhibit limited to no clinical effect [27]. The phase 2 and phase 3 trial failure rates for these compounds is very high with regard to solid tumours. TKIs are referred to as “targeted chemotherapy” drugs but have been shown to actually inhibiting a broad range of targets which can lead to toxicity and tumour resistance [27]. However, lack of target specificity does not completely explain the lack of clinical efficacy. Hence we developed an adaptable model system to investigate the pharmacokinetic uptake of these molecules; we used the registered compounds gefitinib and erlotinib to validate the models applicability [28].

The first major point of the Caco-2 model system is the time in which the monolayers need to be prepared, traditionally this has been a time consuming 21 days. To shorten this we utilized a commercial system from BD Biosciences that required only a 3 day growth period. Monolayers using this system have been shown to have characteristics identical to those grown over 21 days [24]. Initial testing demonstrated several problems using this system for the investigation of gefitinib or erlotinib. It was observed that the donor compartment concentrations were not stable during the course of the experiment showing decreases of 60 % or more of the total drug added to the culture medium.

Investigation into this phenomenon indicated that this was due to the buffer matrix used (HBSS),however, this buffer contained only $Ca^{2+}$ and $Mg^{2+}$ salts and no degradation of the compounds could be observed. Mass spectral analysis of Gefitinib and Erlotinib incubated at 37°C in HBSS buffer suggested that instead a chelation effect was the cause of the loss of concentration. Yamashita et al reported that the relative importance of considering the "physiological conditions of the in vivo drug absorption when optimizing the in vitro experimental conditions". The reference reports that the addition of BSA to the medium improved the transport of high lipophilic drugs with poor medium solubility across the caco-2 monolayer [29]. Both gefitinib and erlotinib are poorly soluble in aqueous solutions and are very highly bound to proteins when circulating in the human system, hence by the simple addition of 5 % BSA we could more closely mimic the "real situation". More importantly 5 % BSA in the medium stabilized the drugs while in solution by preventing "chelation" with the magnesium or calcium ions. This, in turn, yielded more reproducible and accurate permeability characteristics. It should be noted that the addition of transport inhibitors to this protocol did not affect the concentrations of compounds in the initial matrix or after the 3 hour experimental time.

The next issue we observed was due to the sampling technique at individual time points whereby the physical removal of too much of the receiver compartments medium during the experiment led to problems with the monolayer where either a rapid increase or a sharp decline in accumulated transport could be observed on a random basis. The monolayer could not be observed physically but it was reasoned that the observed results were due to either stress breaks or "bubbling effects". The bubbling effect was where air bubbles from sampling procedures had become trapped under the monolayer, isolating the donor compartment from the receiver compartment. This had the consequence of having very high variation between experimental duplicates and inconsistent results on an intra-day basis. Lowering the volume sampled and very careful mixing of a compartment contents reduced this issue down to acceptable parameters. However, sample volume was reduced from 500 µl to 50 µl, requiring the adaptation of the LCMS analytical techniques to be able to utilize only 10-20 µl of sample volume. For gefitinib and erlotinib this proved to be possible.

With experimental parameters optimized a further problem was identified in that the monolayers did not grow consistently across the 24 well plates. Wells in the centre portion of the plate were observed to reach starting experimental conditions much slower than those located on the outer rim of the plate. This created the condition where centrally placed monolayers were just within specifications while outer monolayers were at the maximum limit. This created significant variation in the observed transport characteristics. This issue was solved by isolating each well with a breathable membrane during the entire growth and experimental periods. The resulting protocol was subsequently used to assess transport characteristics of both gefitinib and erlotinib.

Initial investigations demonstrated significant differences in the transport characteristics between gefitinib and erlotinib. Gefitinib demonstrated a 4 fold lower uptake compared to erlotinib when considering the transport in the apical to basolateral direction. However, in the reverse direction erlotinib demonstrated a significantly higher flow whereas for gefitinib it was similar to the apical to basolateral flow. The high flow of erlotinib indicated a potentially large negative flow from the system which would lower its overall bioavailability. To test the applicability of the model system further two active transport inhibitors were used in combination with gefitinib and erlotinib.

Active transport systems dependent on ATP would have been blocked and any difference in transport behaviour would indicate an active transport mechanism for these compounds. The

compound sodium azide inhibits all ATP dependent processes [30]; therefore, if an ATP dependent transporter is involved the total amount accumulated would alter depending on which membrane it was located on and the direction of flow. This model system demonstrated consistent differences between control and inhibited situations indicating that both multiple active and passive transport mechanisms are involved in the uptake of both these compounds. These results also indicate that the polarized membranes of Caco-2 cells had different mechanisms for both uptake and efflux which were different for both compounds. The other inhibitor used was Ko143, a more specific inhibitor of ABCG2 only [31]. This inhibitor also showed differences for both drugs and between apical or basolateral membranes.

For gefitinib, the presence of $NaN_3$ decreased the observed mass transport in the apical to basolateral direction but not completely. This indicated that gefitinib is apparently partially transported by both an active transport mechanism and partly by passive diffusion [7]. Inhibition of ABCG2 seemed to block the drug from accumulating within the cell suggesting that ABCG2 might be one of several transporters involved. However, $NaN_3$ inhibition in the basolateral to apical direction increased gefitinib transported whereas Ko143 decreased the total suggesting the role of another uncharacterized transporter in addition to ABCG2.

Investigation into characteristics of erlotinib demonstrated a different apical to basolateral pattern. Here $NaN_3$ increased slightly the amount transported while Ko143 decreased the total similar to gefitinib in the basolateral to apical directions. However, the total erlotinib transported was significantly higher than gefitinib despite the same starting concentration being used. For erlotinib significantly lower drug accumulation in the cell was detected suggesting that equilibrium between donor and receiver compartments was the driving force of this mechanism with the cellular membrane having little resistance to passive diffusion; it should be considered whether the paracellular route is possibly the predominant mechanisn involved for this compound. Theoretically passive diffusion results in the equilibrium of the compounds between donor, cellular and receiver compartments [32]. However, for erlotinib the most significant of the observed effects is that this concentration gradient is higher in the basolateral (blood) to apical (gut) direction. This could have significant consequences when considered clinically; these results suggest that high single dose schedules would have a better bioavailability compared to regular but lower dosing.

In conclusion we validated a gut epithelial model system to study the potential gut uptake mechanisms for two widely used TKIs, erlotinib and gefitinib. The Caco-2 cell monolayer transwell system with a 3-day culture system proved to be very adaptable to study drug transport and will be very useful to investigating the role of drug transporters using a blocker like probenecid (blocker of ABCC) and verapamil (blocker of ABCB1), that would contribute important overview of drug transporters involved in transport of TKIs.

## Conclusions

In conclusion we validated a gut epithelial model system to study the potential gut uptake mechanisms for two widely used TKIs, erlotinib and gefitinib. The Caco-2 cell monolayer transwell system with a 3-day culture system proved to be very adaptable to study drug transport and will be very useful to investigating the role of drug transporters using a blocker like probenecid (blocker of

ABCC) and verapamil (blocker of ABCB1), that would contribute important overview of drug transporters involved in transport of TKIs.

**References**


[1] E. K. Rowinsky, *Annu. Rev. Med*. **55** (2004) 433-457.

[2] F. Duffaud and C. A. Le Cesne, *Target Oncol*. **4** (2009) 45-56

[3] F. Roszkiewicz, R. Garidi, I. Vaida, B. Royer, A. Parcelier, J. P. Marolleau, and G. Damaj, *Pharmacology* **84** (2009) 38-41.

[4] M. Tolomeo, F. Dieli, N. Gebbia, and D. Simoni, *Anticancer Agents Med. Chem*. **9** (2009) 853-863.

[5] R. L. Comis, *Oncologist*. **10** (2005) 467-470.

[6] N. P. van Erp, H. Gelderblom, and H. J. Guchelaar, *Cancer Treat. Rev*. **35** (2009) 692-706.

[7] M. Galetti, R. R. Alfieri, A. Cavazzoni, M. S. La, M. Bonelli, C. Fumarola, P. Mozzoni, P. G. De, R. Andreoli, A. Mutti, M. Mor, M. Tiseo, A. Ardizzoni, and P. G. Petronini, *Biochem. Pharmacol*. **80** (2010) 179-187.

[8] P. Borst and R. O. Elferink, *Annu. Rev. Biochem*. **71** (2002) 537-592.

[9] C. Lemos, G. Jansen, and G. J. Peters, *Br. J. Cancer* **98** (2008) 857-862.

[10] M. M. Gottesman, T. Fojo, and S. E. Bates, *Nat. Rev. Cancer* **2** (2002) 48-58.

[11] M. Dean, A. Rzhetsky, and R. Allikmets, Genome Res. **11** (2001) 1156-1166.

[12] J. Li, G. Cusatis, J. Brahmer, A. Sparreboom, R. W. Robey, S. E. Bates, M. Hidalgo, and S. D. Baker, *Cancer Biol. Ther*. **6** (2007) 432-438.

[13] Z. Shi, X. X. Peng, I. W. Kim, S. Shukla, Q. S. Si, R. W. Robey, S. E. Bates, T. Shen, C. R. Ashby, Jr., L. W. Fu, S. V. Ambudkar, and Z. S. Chen, *Cancer Res*. **67** (2007) 11012-11020.

[14] Z. Shi, S. Parmar, X. X. Peng, T. Shen, R. W. Robey, S. E. Bates, L. W. Fu, Y. Shao, Y. M. Chen, F. Zang, and Z. S. Chen, *Oncol. Rep*. **21** (2009) 483-489.

[15] C. F. Higgins and M. M. Gottesman, *Trends Biochem. Sci*. **17** (1992) 18-21.

[16] P. Stenberg, U. Norinder, K. Luthman, and P. Artursson, *J. Med. Chem*. **44** (2001) 1927-1937.

[17] R. I. Mahato, A. S. Narang, L. Thoma, and D. D. Miller, *Crit Rev. Ther. Drug Carrier Syst*. **20** (2003) 153-214.

[18] A. T. Heikkinen, T. Korjamo, and J. Monkkonen, *Basic Clin. Pharmacol. Toxicol*. **106** (2010) 180-188.

[19] J. Fogh and G. Trempe, New human tumor cell lines. *In* Human Tumor Cells *In Vitro*. J.Fogh, editor., Plenum Press, New York, (1975) 115-159.

[20] P. H. Vachon and J. F. Beaulieu, *Gastroenterology* **103** (1992) 414-423.

[21] P. Shah, V. Jogani, T. Bagchi, and A. Misra, *Biotechnol. Prog*. **22** (2006) 186-198.

[22] I. J. Hidalgo, T. J. Raub, and R. T. Borchardt, *Gastroenterology* **96** (1989) 736-749.

[23] I. Hubatsch, E. G. Ragnarsson, and P. Artursson, *Nat. Protoc*. **2** (2007) 2111-2119.

[24] S. Yamashita, K. Konishi, Y. Yamazaki, Y. Taki, T. Sakane, H. Sezaki, and Y. Furuyama, *J. Pharm. Sci*. **91** (2002) 669-679.

[25] R. Honeywell, K. Yarzadah, E. Giovannetti, N. Losekoot, E. F. Smit, M. Walraven, J. S. Lind, C. Tibaldi, H. M. Verheul, and G. J. Peters, *J. Chromatogr. B Analyt. Technol. Biomed. Life Sci*. **878** (2010) 1059-1068.

[26] P. R. Wielinga, E. de Waal, H. V. Westerhoff, and J. Lankelma, *J. Pharm. Sci*. **88** (1999) 1340-1347.

[27] F. Broekman, E. Giovannetti, and G. J. Peters, *World J. Clin. Oncol*. **2** (2011) 80-93.

[28] E. Galvani, R. Alfieri, E. Giovannetti, A. Cavazzoni, M. S. La, M. Galetti, C. Fumarola, M. Bonelli, M. Mor, M. Tiseo, G. J. Peters, P. G. Petronini, and A. Ardizzoni, *Curr. Pharm. Des*. **19** (2013) 818-832.

[29] S. Yamashita, T. Furubayashi, M. Kataoka, T. Sakane, H. Sezaki, and H. Tokuda, *Eur. J. Pharm. Sci*. **10** (2000) 195-204.

[30] J. H. Hooijberg, H. M. Pinedo, C. Vrasdonk, W. Priebe, J. Lankelma, and H. J. Broxterman, *FEBS Lett*. **469** (2000) 47-51.

[31] C. Lemos, I. Kathmann, E. Giovannetti, H. Dekker, G. L. Scheffer, C. Calhau, G. Jansen, and G. J. Peters, *Int. J Cancer* **123** (2008) 1712-1720.

[32] C. G. Da Silva, R. J. Honeywell, H. Dekker, and G. J. Peters, *Expert. Opin. Drug Metab Toxicol*. **29** (2015) 1-15.